Detection of Parathyroid Hormone Using an Electrochemical Impedance Biosensor Based on PAMAM Dendrimers

Hakkı Mevlüt Özcan
Chemistry Dept., Faculty of Science, University of Trakya, Edirne, Turkey

Mustafa Kemal Sezgintürk
Chemistry Dept., Faculty of Arts and Sciences, Namık Kemal University, Tekirdağ, Turkey

DOI 10.1002/btpr.2060
Published online February 26, 2015 in Wiley Online Library (wileyonlinelibrary.com)

This paper presents a novel hormone-based impedimetric biosensor to determine parathyroid hormone (PTH) level in serum for diagnosis and monitoring treatment of hyperparathyroidism, hypoparathyroidism and thyroid cancer. The interaction between PTH and the biosensor was investigated by an electrochemical method. The biosensor was based on the gold electrode modified by 12-mercapto dodecanoic (12MDDA). Antiparathyroid hormone (anti-PTH) was covalently immobilized on to poly amidoamine dendrimer (PAMAM) which was bound to a 1-ethyl-3-(3-dimethylaminopropyl)-carbodiimide/N-hydroxysuccinimide (EDC/NHS) couple, self-assembled monolayer structure from one of the other NH_2 sites. The immobilization of anti-PTH was monitored by electrochemical impedance spectroscopy, cyclic voltammetry and scanning electron microscope techniques. After the optimization studies of immobilization materials such as 12MDDA, EDC–NHS, PAMAM, and glutaraldehyde, the performance of the biosensor was investigated in terms of linearity, sensitivity, repeatability, and reproducibility. PTH was detected within a linear range of 10–60 fg/mL. Finally the described biosensor was used to monitor PTH levels in artificial serum samples.
 Biotechnol. Prog., 31:815–822, 2015
Keywords: parathyroid hormone, biosensor, PAMAM, electrochemical impedance spectroscopy, 12-mercapto dodecanoic

Introduction

Parathyroid hormone (PTH), first investigated in early 20th century,[1,2] is a classic hormone that is used worldwide to treat millions of patients with parathyroid disorders. PTH is a polypeptide with 84 amino acids and it tightly regulates calcium and phosphate metabolism in bone, kidneys, intestines and extracellular fluids.[3–5] Even small changes in the PTH level in serum can be an indicator of critical disease of the parathyroid glands such as hyperparathyroidism, which increases PTH level on account of a parathyroid tumor, and hypoparathyroidism which decreases calcium and increases phosphorus level in serum because of lower secretion of PTH.[6–10] Because of this vital importance of sensitive determination of PTH levels, it is crucial to develop methods which are simple, sensitive, and economical. Electrochemical biosensors are seen as being the most promising candidates for the development of novel PTH analysis methods.

Dendrimers are repetitively branched molecules[11,12] and they have lots of advantages in comparison with classical polymers, such as molecular uniformity, stable molecular weight, definite shape, specific size, and lots of surface branches.[13] Poly amido amine (PAMAM) dendrimers are designated "dense star" polymers. They have 11 different generations with 10 functional surface groups. Each new PAMAM generation is fabricated around the preceding generation with a series of repetitive groups. Finally, the new generation of PAMAM has new features such as larger diameter, larger molecular weight and more reactive surface branches. PAMAM has a unique property with the reactive surface branches which allow many alternations to be made to the surface. PAMAM dendrimers have very strong potential to be used as affinity ligands, radioligands, detecting agents, targeting components or pharmaceutically active compounds, due to their convertible surface.[14–16]

Electrochemical impedance spectroscopy (EIS) is a highly sensitive indicator of a wide variety of biochemical and physical properties and provides an effective method to probe the electric features of surface-modified electrodes with ultrahigh sensitivity. Therefore, EIS has been used to fabricate a great number of biosensors and to monitor enzyme reactions and relationships between specific molecules, such as proteins, receptors, nucleic acids, antibodies, and whole cells[17,18] Some research groups have reported impedimetric biosensors based on self-assembled monolayers (SAM).[19–23] Some research regarding the use of 12 mercapto dodecanoicacid (12MDDA) for the purpose of forming SAM has been reported.[24–26] Application of SAMs to biosensor surfaces have many advantages such as forming a highly ordered unimolecular film, flexibility to design different head

Additional Supporting Information may be found in the online version of this article.

Correspondence concerning this article should be addressed to H. M. Özcan at ozcanhakki@gmail.com.

groups of monolayers by a large number of electroactive or electroinactive functional groups, and hydrophobic and hydrophilic groups at the end of the monolayers provide an excellent way to immobilize different types of molecules. Although these are important advantages, SAMs also have some disadvantages, such as the lack of chemical stability of some SAMs, negative effects of electrical field and thermal desorption on biosensor applications, and unwanted adsorption of contaminants.[25]

Recently various EIS-based biosensors have been described, such as phenomena of polymer degradation, magnetic nanobeads, nanometer-sized hydroxyapatite, and molecular imprinted polymers.[27–30]

The objective of this study is to develop an EIS-based electrochemical biosensor system to determine PTH sensitively, practically and promptly. The biological significance of PTH levels in serum makes our biosensor more important for use in the determination of PTH because the biosensor presented enables detection of PTH levels in serum accurately and sensitively. An SAM strategy for introducing an immobilization platform on the gold electrodes is reported in this study. 12MDDA was used to form SAM. Anti-parathyroid hormone (anti-PTH) was covalently attached to the SAM of PAMAM by means of glutaraldehyde and the couple of 1-ethyl-3-(3-dimehylaminopropyl) carbodiimide (EDC) and *N*-hydroxysuccinimide (NHS). EIS was used to determine the diffusion rate of the redox probe associated with changes in the electron transfer resistance (ΔR_{ct}) related to PTH concentration. The proposed biosensor can detect concentrations of PTH at very low levels. We also identified scanning electron microscopy (SEM) features of the surfaces of each layer based on a combination of EIS in the presence of $[Fe(CN)_6]^{3-/4-}$ as a redox couple. Finally, artificial serum samples spiked with PTH were analyzed with the biosensor.

Experimental

Materials and instrumentation

All reagents were of analytical grade and were purchased from Sigma-Aldrich (St. Louis, MO). PTH and anti-PTH were portioned at certain concentrations and were stored at −20°C until use. Artificial serum solution was prepared using 5 mM $CaCl_2$,4.5 mM KCl, 1.6 mM MgCl, 4.7 mM D(+) glucose, 0.1% human serum albumin, 2.5 mM urea, and 145 mM NaCl. A three-electrode system, consisting of an Ag/AgCl (saturated KCl) reference electrode, a Pt counter-electrode, and a gold working electrode (with a surface area of 2.01 mm^2), was housed in a 5-mL electrochemical cell (all electrodes were obtained from m BASi, Warwickshire, UK). Electrochemical experiments were performed using a Gamry Interface 1000 Potentiostat/Galvanostat, (Gamry Instruments, Warminster, USA) interfaced with a PC via EChem Analyst containing cyclic voltammetry (CV) and EIS softwares (Gamry Instruments, Warminster, USA).

Modification of the gold electrodes by 12MDDA SAM

Before use, the gold electrodes were first polished with 0.05 μm alumina powder and then washed with ultrapure water. Following that the electrodes were ultrasonically washed in absolute ethanol for 3 min to remove alumina residues. Then the surfaces of the electrodes were dried by a pure argon stream. This polishing and cleaning procedure was repeated before every electrode preparation step. The clean gold electrodes were immediately immersed into 12MDDA solution (5 mM, in pure ethanol) for 16 h. After this period, they were rinsed with ethanol and gently dried with an argon stream.

Anti-PTH attachment on 12MDDA modified electrodes

For anti-PTH immobilization, EDC was used as a heterobifunctional crosslinker. NHS was used in conjunction with the crosslinker, PAMAM was used as an increasing agent for the active terminal, and glutaraldehyde (GLT) was used to activate the amino ends of the PAMAM. EDC/NHS solution (0.1 M EDC, 0.05 M NHS) was spread over the electrode surface, and was then left for 30 min in a dark ambient environment. Later, gold electrodes were washed with ultrapure water gently and then dried by pure argon stream again. For the next step, PAMAM (1.5%) was dropped on to the electrode surface, and was then left for 60 min. Afterwards, GLT (1%) was spread over the electrode surface, and was then left for 15 min. At the end of the each step electrodes were washed with ultrapure water gently and then dried by pure argon stream again. Then 5 μL of anti-PTH portion was applied to the active electrode surface by a pipette. The electrode was allowed to incubate for an hour in a moist medium. Finally, the electrode was immersed into ultrapure water to remove physically adsorbed anti-PTH molecules. Bare gold electrodes and the modified electrodes were denoted as Au, Au/12MDDA, Au/12MDDA/EDC–NHS, Au/12MDDA/EDC–NHS/PAMAM, Au/12MDDA/EDC–NHS/PAMAM/GLT, Au/12MDDA/EDC–NHS/PAMAM/GLT/AntiPTH, and Au/12MDDA/EDC–NHS/PAMAM/GLT/AntiPTH/PTH.

Electrochemical studies

CV was used to characterize SAM formation on bare gold electrodes. The potential was varied between −0.5 and 1 V (step size: 20 mV, scan rate: 50 mV/s) in the presence of 5 mM $K_3[Fe(CN)_6]/K_4[Fe(CN)_6]$ (1:1) solution which served as a redox probe containing 0.1 M KCl. For EIS studies, an alternating wave with amplitude of 10 mV was applied to the electrode. In the potentiostatic mode, EIS experiments were done at a fixed DC potential of 0 V. The redox couple used for EIS was the same as that used for CV. Impedance spectra were obtained in the frequency range between 10,000 and 0.05 Hz.

Working principle of the biosensor

Firstly a PTH standard solution or sample was injected onto the biosensor surface by a micropipette. The injection volume was 5 μL. The biosensor then was incubated in a moist medium for 60 min. At the end of this period, the biosensor was washed in ultrapure water to remove physically adsorbed PTH molecules. The biosensor was again put into the electrochemical cell containing $Fe(CN)_6^{4-/3-}$ redox probe solution and the electrochemical measurements were taken. The difference in charge transfer resistance between before and after injection of PTH was used to create PTH calibration curves.

Scanning electron microscopy (SEM) investigations

Structural observations of the surface modified by immobilization and PTH binding were performed by a field

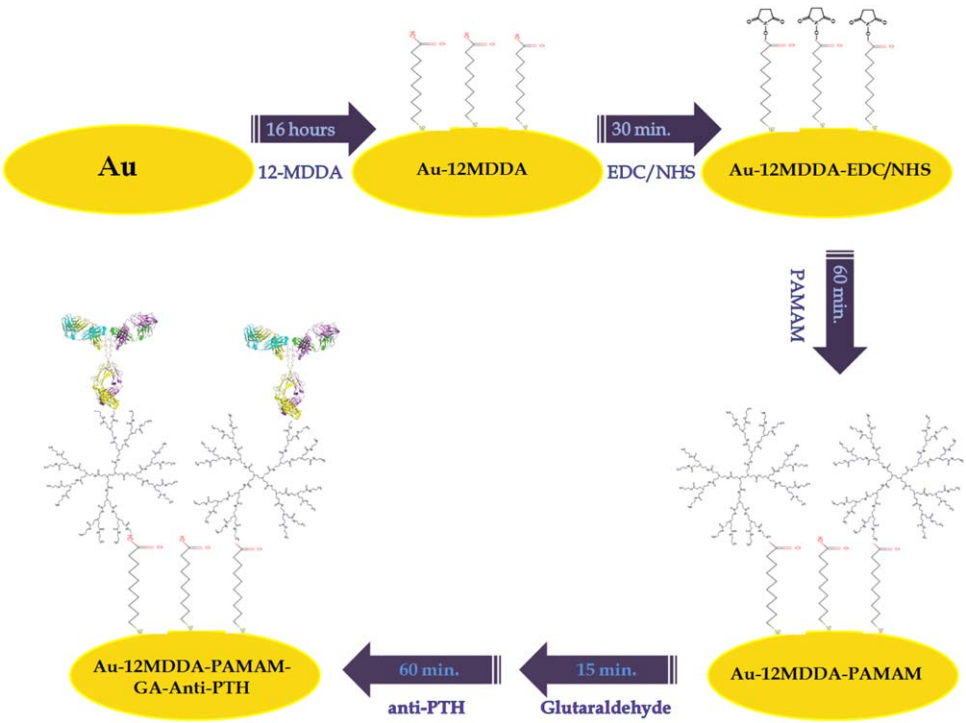

Figure 1. Schematically representation of the fabrication of PAMAM based biosensor.

emission scanning electron microscope (FEI-Quanta FEG 250 model at 10,000-fold magnification) at the Scientific and Technological Research Center of Namık Kemal University (NABİLTEM). An acceleration voltage of 5 kV was used to acquire SEM images.

Results and Discussion

Anti-PTH immobilization

The first step of antiPTH immobilization was adsorbtion of 12MDDA onto the gold electrode surface spontaneously. The adsorbtion of thiols molecules bonds to gold extraordinarily strongly. The second step was activating the carboxyl ends of 12MDDA which was performed with the help of the frequently used EDC/NHS chemistry. In this way, the amine-cored PAMAM dendrimers were covalently attached onto the gold electrode surface. In the final step, GLT was used as a crosslinker agent between PAMAM and anti-PTH. All of these steps are summarized in Figure 1.

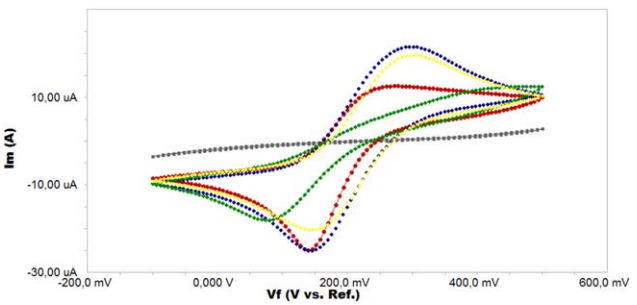

Figure 2. Electrochemical characterization of PAMAM based anti-PTH biosensor [cyclic voltammograms related with anti-PTH immobilization by covalently attachment [-◆-◆-(yellow): bare gold electrode, -■-■-(gray):12MDDA, -•-•-(red):12MDDA-EDCNHS, -◆-◆-(blue): 12MDDA-EDCNHS-PAMAM, -◆-◆-(green): 12MDDA-EDCNHS-PAMAM-GLT-Anti-PTH].

The layer by layer formation of the biosensors was characterized by EIS and CV. Because $K_3[Fe(CN)_6/K_4[Fe(CN)_6]$ was very sensitive to surface modifications, it was preferred for use as an electrochemical probe in the experiments. Electrochemical impedance spectra were significantly affected by modifications on the electrode surface. EIS consists of resistive and capacitive elements besides the Warburg element and is a powerful method for analyzing the complex electrical resistance of a system. EIS is also sensitive to surface characteristics and changes in bulk properties; moreover, it is especially well-suited to the detection of binding events on the transducer surface in biosensor fields; therefore it is a valuable and progressive technique.

The cyclic voltammograms and EIS spectra of each immobilization step of the anti-PTH are shown in Figures 2 and 3. Each immobilization step is well defined by redox couple. When the electrode was covered by the 12MDDA (SAM), as seen in Figure 3 charge–transfer resistance (R_{ct}) was highly increased because the carboxyl groups of 12MDDA probably prevented the negatively-charged ferricyanide from reaching the electrode surface. As shown in Figure 2, the characteristic CV peaks of the electrode could not been seen after 12MDDA modification of the electrode surface because it became dielectric. The relatively long alkyl chain of 12MDDA showed a highly ordered monolayer on the surface due to van der Waals interactions between the R–S units. Moreover, it is known that the thermodynamic stability of SAMs increases with the length of the alkyl chain.

After the EDC/NHS couple was reacted with 12MDDA, R_{ct} was observed to be under 4.0 kΩ (Figure 3). The reason is that when the carboxyl groups of 12MDDA were activated by positively charged EDC/NHS couples, the negatively charged redox probes were adsorbed by the surface of

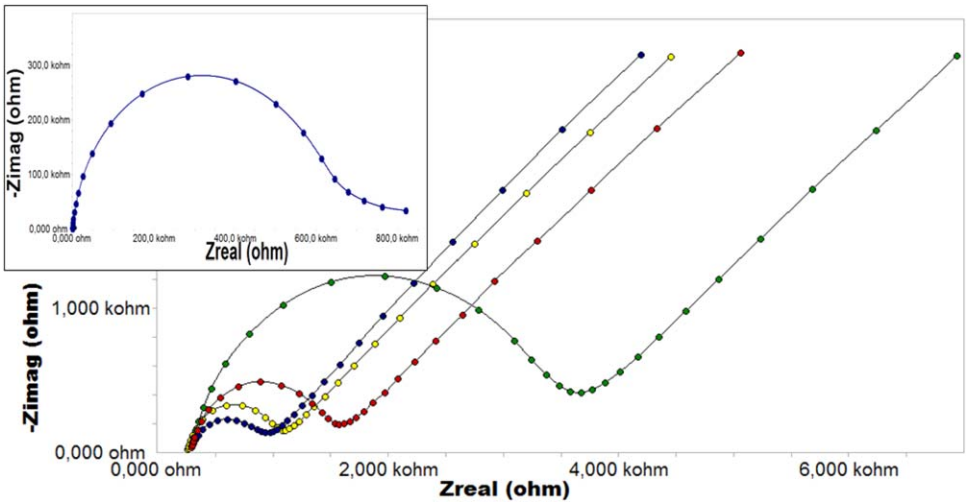

Figure 3. Electrochemical impedance spectra of anti-PTH immobilization steps [inset figure: 12MDDA, -•-•- (yellow): bare gold electrode, -•-•- (red):12MDDA-EDCNHS, -•-•- (blue): 12MDDA-EDCNHS-PAMAM, -•-•- (green): 12MDDA-EDCNHS-PAMAM-GLT-Anti-PTH].

electrode. Therefore, the characteristic CV peaks of the conductor surface could be seen. Amino groups of PAMAM are positively charged at pH = 7. After the PAMAM modification of the surface, the further positively charged groups absorbed the negatively charged ferricyanide to the electrode surface. Just as expected, the electrostatic interactions take place between negatively charged redox probe and the positively-charged primary amino groups on the PAMAM. Consequently the R_{ct} was decreased. Similarly when the R_{ct} was decreased, the CV peak increased because of the high current.

Covalent immobilization of anti-PTH on the surface enhanced the insulating property of the electrode surface and this resulted in an increase of R_{ct} and decrease of CV peak, which could be seen in cyclic voltammograms and EIS spectra. This could be explained because the modification by PAMAM of the surface may increase the effective area of the electrodes, and surface coverage of anti-PTH molecules improved, so the electrochemical detection signals for PTH should increase considerably. Moreover, PAMAM dendrimers also have some important advantages such as easily spreading on different surfaces to form films,[31] they tend to form densely packed film which maintains lower surface tension.[32] Most importantly, PAMAM dendrimers introduce an excess of active ends which can be used for the immobilization of any bioreceptor molecules.

SEM investigations

To monitor the construction of the biosensor and the binding of PTH we used a scanning electron microscope. The SEM images are given in Figure 4A–E. Figure 4A shows Au (bare electrode), Figure 4B shows the image after 12MDDA modification (Au-12MDDA), Figure 4C shows

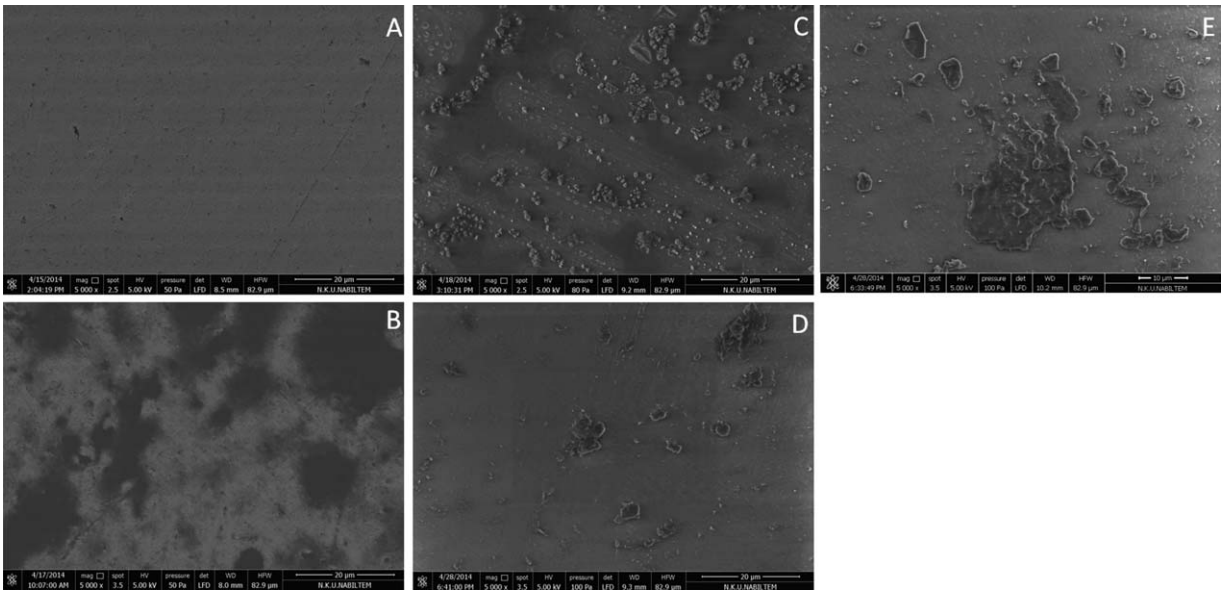

Figure 4. SEM investigations of the biosensor surfaces.

[SEM images: (A) bare gold electrode, (B) 12MDDA, (C) 12MDDA-EDCNHS-PAMAM, (D) Au-12MDDA-EDCNHS-PAMAM-$NaBH_4$-GLT-Anti-PTH, (E) Au-12MDDA-EDCNHS-PAMAM-$NaBH_4$-GLT-Anti-PTH-PTH].

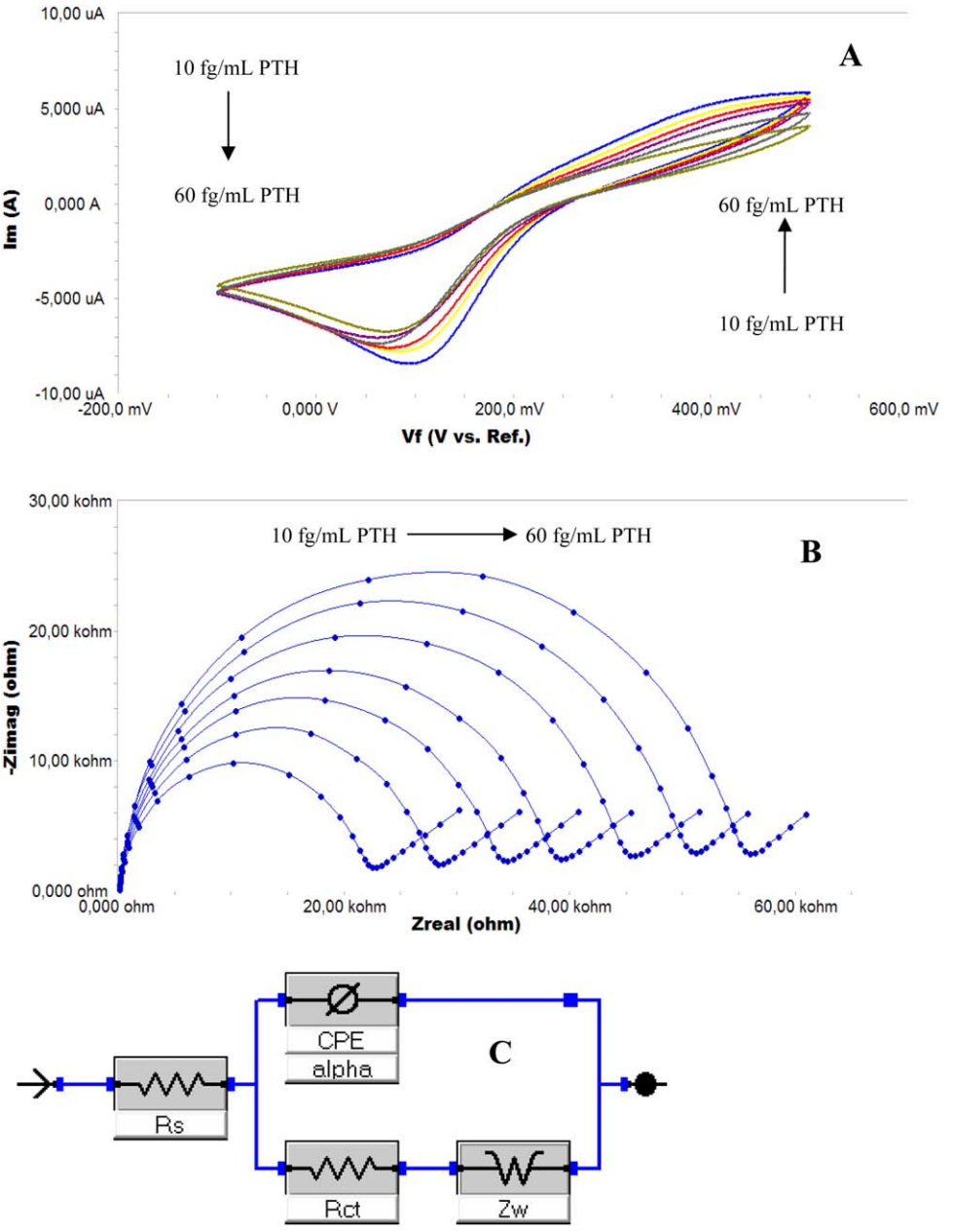

Figure 5. Cyclic voltammograms (A), impedance spectrums (B) obtained for different concentrations of Parathyroid Hormone by PAMAM based anti-PTH biosensor.

the image after PAMAM modification (Au-12MDDA-EDCNHS-PAMAM), Figure 4D shows the image after anti-PTH immobilization (Au-12MDDA-EDCNHS-PAMAM-GLT-Anti-PTH), and Figure 4E shows the image after PTH binding (Au-12MDDA-EDCNHS-PAMAM-GLT-AntiPTH-PTH). Figure 4A shows the surface of a typical gold electrode. The surface topography showed good definition of smooth gold surface. Figure 4B shows that the covering of the surface by 12MDDA SAM resulted in a cloudlike appearance. PAMAM modification can be obviously seen in Figure 4C. PAMAM molecules look like clusters of flower-like spheres with submicron sizes. Figure 4D shows that the immobilization of anti-PTH caused in a sponge-like, porous structure on the electrode surface. Following the injection of PTH solution, the morphology of the biosensor surface underwent a change (Figure 4E). The sponge-like structures are obviously bigger than that shown in Figure 4D. Moreover, this result could be attributed to the interaction of anti-PTH and PTH.

Optimization of the biosensor

Layer-by-layer preparation of the biosensor was examined in terms of the effect of 12MDDA concentration, EDC/NHS couple concentration, PAMAM concentration, GLT concentration, and anti-PTH concentration. Details are given below:

In order to explain the effect of 12MDDA concentration on the response of the biosensor, 5–30 pg/μL PTH standard solutions were separately analyzed by biosensors prepared with different concentrations of 12MDDA (2.5, 5, 7.5, 10 mM). As seen in Supporting Information Figure S1, R^2 values were calculated as 0.9610, 0.9981, 0.9882, and 0.9755, respectively. Also, 20 pg/μL PTH standard solution was separately analyzed by different biosensors for the

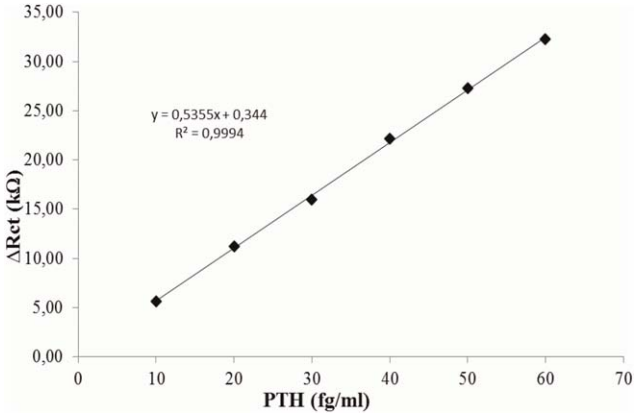

Figure 6. PTH calibration curve obtained by the present PAMAM based biosensor.

investigation of 12MDDA concentration on R_{ct}. The spectra of the experiments are given in Supporting Information Figure S2. R_{ct} values were 7.852, 17.11, 19.18, and 22.76 kΩ, respectively. This increase in R_{ct} values with increasing 12MDDA covering was expected. Higher concentrations of 12MDDA resulted in an increase of R_{ct} value, probably because the density of surface covering increased and blocked electron transfers. Although the highest R_{ct} value was found at 10 mM 12MDDA concentration, according to the linearities of the biosensors, optimum 12MDDA concentration was determined as 5 mM and this was used for all of the experiments after this step.

The next step in the optimization studies was concentration of the NHS/EDC couple. For this purpose 75–37.5, 100–50, 150–75, and 200–100 mM NHS/EDC couple concentrations were used for the construction of biosensors. 5–30 pg/μL PTH standard solutions were separately analyzed by biosensors for the investigation of the linearity of biosensor responses, and also 20 pg/μL PTH standard solutions were separately analyzed by different biosensors for the purpose of comparing R_{ct} values. As seen in Supporting Information Figure S3, R^2 values were calculated as 0.9632, 0.9928, 0.9821, and 0.9872, respectively, while R_{ct} values were 39.86, 34.11, 32.11, and 15.00 kΩ, respectively. The 200—100 mM NHS/EDC couple concentration resulted in the lowest R_{ct} value. The impedance spectra are given in Supporting Information Figure S4. This situation was expected because the EDC/NHS couple had increased the conductivity of the surface. But the increase in the concentration of the EDC/NHS couple led to further immobilization of anti-PTH and also PTH; subsequently the SAM could not carry this weight. Therefore the linearity of the biosensor responses declined. The 100–50 mM EDC/NHS couple concentration was chosen as the optimal concentration because of this response profile.

The biosensors were prepared by using 0.5, 1.0, 1.5, and 2.0% PAMAM solutions in optimization studies of the PAMAM concentration. For this aim, the experiments were done under the same conditions described above. As can seen in Supporting Information Figure S5, R^2 values were calculated as 0.9660, 0.9542, 0.9778, and 0.9024, respectively, while R_{ct} values were 7.21, 9.23, 11.02, and 11.85 kΩ, respectively, given in Supporting Information Figure S6. At the higher PAMAM concentrarions (1.5 and 2.0%) R_{ct} values were almost the same. Because of the linear response of the biosensor, the 1.5% PAMAM solution was chosen as the optimum PAMAM concentration. For the next step, the biosensors were prepared with different GLT concentrations (0.5, 1.0, and 1.5%) to determine the optimum GLT concentration. For this purpose, the experiments were carried out with the same conditions described above. R^2 and R_{ct} values are given in Supporting Information Figures 7 and 8, respectively. R^2 were calculated as 0.9901, 0.9869, and 0.9685, respectively, while R_{ct} values were 17.63, 21.35, and 22.29 kΩ, respectively. According to the response linearity and R_{ct} values, the 1.0% GLT solution was chosen as optimum GLT concentration.

In the last step of the optimization studies, the effect of the anti-PTH concentration on the biosensor response was investigated. For this aim, biosensors were prepared with different concentrations of anti-PTH (10, 25, 50, 75, 100, 150, and 200 ng/5μL) and used for analysis of 5–30 pg/μL PTH standards. As seen in Supporting Information Figure S9, R^2 values were calculated as 0.8842, 0.9732, 0.9717, 0.9881, 0.9919, 0.9525, and 0.9770, respectively. Higher concentrations of anti-PTH (150 and 200 ng/5 μL) resulted in denser bond between PTH and anti-PTH. Therefore, the higher anti-PTH concentration leads to higher R_{ct} value. This stituation was expected, but the denser bond between PTH and anti-PTH could probably lead to deformation of surface. Hence, the linearity of response was damaged. According to the response linearity and R_{ct} values, the 100 ng/5 μL anti-PTH concentration was chosen as the optimum concentration.

Analytical characteristics of the biosensor

The described biosensor was characterized with regard to its linear range, reproducibility, and repeatability. In this study, EIS was successfully used to determine the amount of PTH on the electrode surface associated with changes in the

Table 1. Comparison of the Developed Methods for PTH Determination

Type	Immobilization Technique	Measurement Principle	Linear Detection Ranges	References
CTK (Q-IntraOperative Intact PTH)	Bead	Chemiluminescence	6–1250 (pg/mL)	34
CTK (TurboIntact PTH)	Bead	Chemiluminescence	4–2500 (pg/mL)	34
CTK (STAT-IO-I-PTH)	Microtite strips With Accusphere	Chemiluminescence	6–2500 (pg/mL)	34
CTK (Elecsys PTH)	Microparticals	Electro Chemiluminescence	1.2–5000 (pg/mL)	34
CTK (ARCHITECT)	Microparticals	Chemiluminescence	0.5–1886 (pg/mL)	35
CTK (LIAISON)	Two-site sandwich	Chemiluminescence	7.1–1958 (pg/mL)	35
Research Article	M.Partical (300nm)	Giant magneto-resistive	95-NL (pg/mL)	33
Research Article	M.Partical (500nm)	Giant magneto-resistive	7.6-NL (pg/mL)	33
Research Article	Cell	Time-resolved fluorescence	3.75–9.38 (pg/mL)	36
DescribedArticle	PAMAM	Impedance spectroscopy	10–60 (fg/mL)	–

CTK, commerical test kit; NL, not limited

Table 2. Reproducibility and Serum Samples Analyses Studies for the Biosensor

The reproducibility experiment results of the biosensor			
Biosensor Numbers	R^2	y	Linear Ranges (fg/mL)
1	0.9955	$0.8087x + 11.685$	10–60
2	0.9929	$0.6078x + 0.7913$	10–60
3	0.9914	$0.6263x - 1.5133$	10–60
4	0.9958	$0.9563x + 3.6967$	10–60
5	0.9870	$0.7121x + 3.1220$	10–60
6	0.9991	$0.9255x + 0.6850$	10–60
7	0.9994	$1.5176x + 3.6129$	10–60
8	0.9941	$1.6048x - 2.4240$	10–60
9	0.9982	$1.5235x + 2.1160$	10–60
10	0.9924	$1.4171x - 1.5241$	10–60
PTH detection in artificial serum samples by the presented biosensor			
Added PTH (fg/mL)	Found by Biosensor (fg/mL)	Recovery (%)	Relative Differences (%)
10	9.832	98.32	1.68
20	20.520	102.60	2.60
30	28.680	95.60	4.40
40	39.344	98.36	1.64
50	48.71	97.42	2.58

R_{ct} of the biosensor. To obtain a linear relation between PTH concentrations and electrochemical signals, the absolute impedance values were used. The impedance values were extracted by using an equivalent circuit model as shown in Figure 5C. In this model C_{pe} is the double layer capacitance of the system, R_{ct} refers the charge transfer resistance in low frequency, Z_w is the Warburg element, and R_s shows the resistance of the electrolyte and all the connections. A simple equation: $\Delta R_{ct} = R_{ct(PTH)} - R_{ct(anti\text{-}PTH)}$ was used to calculate the impedance changes, where $R_{ct(PTH)}$ is the value of the charge transfer resistance after anti-PTH is coupled with PTH, while $R_{ct(anti\text{-}PTH)}$ is the value of the charge transfer resistance when anti-PTH is immobilized on the electrode surface. As can be seen from Figure 5A, peak currents decreased with an increase in the concentration of PTH standard solutions.

Nyquist plots of the developed biosensor for different PTH concentrations are shown in Figure 5B. It was seen that increasing PTH concentration led to an increase the semicircle diameter in the Nyquist plots. Moreover, concentration-dependent analysis can be performed at low frequencies. The increment of PTH concentration increased the charge transfer resistance, achieving a linear range between 10 and 60 fg/mL. The results revealed that the presented biosensor allowed determination of PTH in an extremely sensitive manner. A standard calibration graph for PTH was drawn with the help of the changes in R_{ct} after PTH applications. Figure 6 shows the calibration curve.

A magnetic particle-based immunoassay for the detection of PTH was reported.[33] To monitor the PTH concentration, a detection limit in the 95 pg/mL range was obtained with 300 nm particles. When 500 nm particles were used, 7.6 pg/mL of PTH was detectable. Also Sokoll et al. described a cell-based immunoassay for detection of PTH and they achieved a linear range between 3.75 and 9.38 60 pg/mL.[34] Some commercially available immunoassay (EIA) test kits can be frequently used by laboratories. These products are *in vitro* quantitative assays for detecting PTH based on the principle of competitive enzyme immunoassay. The minimum detectable concentration of PTH is 0.5 pg/mL. Certain commercial detection tools and the methods mentioned above are summarized in Table 1. The lowest PTH concentration, a limit of detection (LOD), has also been calculated as 1.43 fg/mL by the general equation [k, S_{blank}/m], where $k-3$, S_{blank} and m represent impedance signals obtained for blank sample and the slope, respectively. The limit of quantification (LOQ) was also obtained by taking $k-10$ in the above equation. LOQ for the biosensor was calculated as 4.78 fg/mL. LOD and LOQ values indicated that the proposed biosensor could be used for sensitive determination of PTH.

The repeatability of the immunosensors was examined by analysis of the same concentration of PTH (30 fg/mL) using five similarly prepared electrodes. The five immunosensors, made independently, showed the changes in impedance responses of 33.85, 30.96, 32.41, 29.25, and 30.77 kohm. It was observed that the immunosensor had good repeatability with a relative standard deviation of 1.74% (less than 5.0%).

The reproducibility of the presented anti-PTH biosensor was approved by using different biosensors fabricated via the same set of procedures for PTH analysis 10 times. As is known, the definition of reproducibility is the same for electrochemical biosensors as for any other analytical device. Reproducibility is a measure of the scatter or the drift in a series of observations or results performed over a period of time. It is generally determined for the analyte concentrations within the usable range. The results showed that the developed biosensor reported here can be reproducibly used for PTH detection and quantification. The linear detection ranges of 10 biosensors for PTH were the same: between 10 and 60 fg/mL. The results can be seen in Table 2.

Additionally, the biosensor was used for artificial serum samples spiked with PTH. The results of five different measurements can also be seen in Table 2. The results presented here showed that PTH levels of the artificial serum samples analyzed by the present biosensor agreed with the spiked amount in the artificial serum samples.

Conclusion

In conclusion, we report a simple electrochemical biosensor for detection of PTH with ultrahigh sensitivity measurement, which could be an effective method for characterization of the interaction between PTH and anti-PTH. Clearly, the development of a reliable device for PTH

monitoring is an important goal that will have great impact on the clinical management of PTH-related diseases. The immobilization of anti-PTH on 12MDDA with PAMAM-modified gold electrodes was significantly simple and effective. The biosensor was characterized by CV and EIS in detail. The proposed biosensor is highly reproducible and is able to detect PTH in a linear range of 10–60 fg/mL. Although this presents advantages, future generations of this and other PTH detection methods should be rigorously evaluated for accuracy and reproducibility in real-life clinical settings before release for general use.

Acknowledgment

Support from Trakya University Scientific Research Foundation (Project Number: TUBAP-2001/195) and TÜBİTAK (The Scientific and Technological Research Council of Turkey, Project number: 113 Z 678) are gratefully acknowledged.

Literature Cited

1. Boothby WM. The parathyroid glands: a review of the literature. *J Endocrinol*. 1921;5:403–440.
2. Collip JB. The extraction of a parathyroid hormone which will prevent or control parathyroid tetany and which regulates the level of blood calcium. *J Biol Chem*. 1925;63:395–438.
3. Brown EM. Homeostatic mechanisms regulating extracellular and intracellular calcium metabolism. In: Bilezikian JP, Levine MA, Marcus R, edıtors. *The Parathyroids*. New York: Raven Press; 1994:15–54.
4. Martin TJ. Does bone resorption inhibition affect the anabolic response to parathyroid hormone? *Trends Endocrinol Metab*. 2004;15:49–50.
5. Murray JF. *Primer on the Metabolic Bone Diseases and Disorders of Mineral Metabolism*. Washington DC: American Society for Bone and Mineral Research Publication; 2003.
6. Palazzo FF, Delbridge LW. Minimal-access/minimally invasive parathyroidectomy for primary hyperparathyroidism. *Surg Clin North Am*. 2004; 84: 717–734.
7. Kairys JC, Daskalakis C, Weigel RJ. Surgeon-performed ultrasound for preoperative localization of abnormal parathyroid glands in patients with primary hyperparathyroidism. *World J Surg*. 2006;30:1658–1664.
8. Coker LH, Rorie K, Cantley L, Kirkland K, Stump D, Burbank N, Tembreull T, Williamson J, Perrier N. Primary hyperparathyroidism, cognition, and health-related quality of life. *Ann Surg*. 2005;242:642–650.
9. Shoback D. Clinical practice hypoparathyroidism. *N Engl J Med*. 2008;359:391–403.
10. Cañadillas S, Canalejo A, Santamaría R. Calcium-sensing receptor expression and parathyroid hormone secretion in hyperplastic parathyroid glands from humans. *J Am Soc Nephrol*. 2005;16:2190–2197.
11. Astruc D, Boisselier E, Ornelas C. Dendrimers designed for functions: from physical, photophysical, and supramolecular properties to applications in sensing, catalysis, molecular electronics, and nanomedicine. *Chem Rev*. 2010;110:1857–1959.
12. Vögtle F, Richardt G, Werner N. Dendrimer chemistry concepts, syntheses, properties, applications. Weinheim: WILEY-VCH Verlag GmbH & Co. KGaA; 2009.
13. Morgan MT, Nakanishi Y, Kroll DJ, Griset AP, Carnahan MA, Wathier M, Oberlies NH, Manikumar G, Wani MC, Grinstaff MW. Dendrimer-encapsulated camptothecins: increased solubility, cellular uptake, and cellular retention affords enhanced anticancer activity *in vitro*. *Cancer Res*. 2006;66:11913–11921.
14. Tekade RK, Dutta T, Gajbhiye V, Jain NK. Exploring dendrimer towards dual drug delivery. *J Microencapsul*. 2009;26:287–296.
15. Fernandes EGR, Vieira NCS, de Queiroz AAA, Guimaraes FEG, Valtencir Z. Immobilization of poly(propylene imine) dendrimer/nickel phthalocyanine as nanostructured multilayer films to be used as gate membranes for SEGFET pH sensors. *J Phys Chem C*. 2010;114:6478–6483.
16. Campos BB, Manuel A, da Silva E, Joaquim CG. Fluorescent properties of a pybrid cadmium sulfide-dendrimer nanocomposite and its quenching with nitromethane. *J Fluoresc*. 2010;20: 143–151.
17. Guan JG, Miao YQ, Zhang QJ. Impedimetric biosensors. *J Biosci Bioeng*. 2004;97:219–226.
18. Katz E, Willner I. Probing biomolecular ınteractions at conductive and semiconductive surfaces by ımpedance spectroscopy: routes to ımpedimetric ımmunosensors, DNA-sensors, and enzyme biosensors. *Electroanalysis*. 2003;15:913–947.
19. Bott AW. Electrochemical techniques for the characterization of redox polymers. *Curr Sep*. 2001;19:71–75.
20. Hsieh KM, Lan KC, Hu WL, Chen MK, Jang LS, Wang MH. Glycated hemoglobin (HbA_{1c}) affinity biosensors with ring-shaped interdigital electrodes on impedance measurement. *Biosens Bioelectron*. 2013;49:450–456.
21. Sonuç MN, Sezgintürk MK. Ultrasensitive electrochemical detection of cancer associated biomarker HER3 based on anti-HER3 biosensor. *Talanta*. 2014;120:355–361.
22. Sezgintürk MK, Uygun ZO. An impedimetric vascular endothelial growth factor biosensor-based PAMAM/cysteamine-modified gold electrode for monitoring of tumor growth. *Anal Biochem*. 2012;423:277–285.
23. Huang IY, Lee MC. Development of a FPW allergy biosensor for human IgE detection by MEMS and cystamine-based SAM technologies. *Sens Actuat B Chem*. 2008;132:340–348.
24. Wink T, Van Zuilen SJ, Bult A, Van Bennekom WP. Self-assembled monolayers for biosensors. *Analyst*. 1997;122:43–50.
25. Chaki NK, Vijayamohanan K. Self-assembled monolayers as a tunable platform for biosensor applications. *Biosens Bioelectr*. 2002;17:1–12.
26. Yoon M, Hwang HJ, Kim JH. Immobilization of antibodies on the self-assembled monolayer by antigen-binding site protection and immobilization kinetic control. *J Biomed Sci Eng*. 2011;4:242–247.
27. Fernández-Sánchez C, McNeil CL, Rawson K. Electrochemical impedance spectroscopy studies of polymer degradation: application to biosensor development, TrAC. *Trends Anal Chem*. 2005;24:37–48.
28. Fredj HB, Helali S, Esseghaier C, Vonna L, Vidal L, Abdelghani A. Labeled magnetic nanoparticles assembly on polypyrrole film for biosensor applications. *Talanta*. 2008;75:740–747.
29. Yang L, Wei W, Gao X, Xia J, Tao H. A new antibody immobilization strategy based on electrodeposition of nanometer-sized hydroxyapatite for label-free capacitive immunosensor. *Talanta*. 2005;68:40–46.
30. Panasyuk-Delaney T, Mirsky VM, Ulbricht M, Wolfbeis OS. Impedometric herbicide chemosensors based on molecularly imprinted polymers. *Anal Chim Acta*. 2001;435:157–162.
31. Tsukruk VV, Rinderspacher F, Bliznyuk VN. Self-assembled multilayer films dendrimers. *Langmuir*. 1997;13:2171–2176.
32. Li J, Piehler LT, Qin D, Baker Jr JR, Tomalia DA, Maier DJ. Visualization and characterization of poly(amidoamine) dendrimers by atomic force microscopy. *Langmuir*. 2000;16:5613–5616.
33. Dittmer WU, de Kievit P, Prins MWJ, Vissers JLM, Mersch MEC, Martens MFWC. Sensitive and rapid immunoassay for parathyroid hormone using magnetic particle labels and magnetic actuation. *J Immunol Methods*. 2008;338:40–46.
34. Sokoll LJ, Wians FH, Remaley AT. Rapid ıntraoperative immunoassay of parathyroid hormone and other hormones: a new paradigm for point-of-care testing. *Clin Chem*. 2004;50:1126–1135.
35. La'ulu SL, Roberts WL. Performance characteristics of six ıntact parathyroid hormone assays. *Am J Clin Pathol*. 2010;134: 930–938.
36. Hohensteina A, Hebell M, Zikry H, El Ghazaly M, Mueller F, Rohde J. Development and validation of a novel cell-based assay for potency determination of human parathyroid hormone (PTH). *J Pharmacol Biomed Anal*. 2014;98:345–350.

Manuscript received Jul. 21, 2014, and revision received Dec. 19, 2014.